THE UNIVERSITY of EDINBURGH

Edinburgh Research Explorer

In Vivo Study of Naturally Deformed Escherichia coli Bacteria

OPEN ACCESS

In Vivo Study of Naturally Deformed *Escherichia coli* Bacteria

Sharareh Tavaddod · **Hossein Naderi-Manesh**

Abstract A combination of light-microscopy and image processing has been applied to study naturally deformed *Escherichia coli in vivo* condition and at the order of sub-pixel high-resolution accuracy. To classify deflagellated non-dividing *E. coli* cells to the rod-shape and bent-shape, a geometrical approach has been applied. From the analysis of the geometrical data which were obtained of image processing, we estimated the required effective energy for shaping a rod-shape to a bent-shape with the same size. We evaluated the energy of deformation in the naturally deformed bacteria with minimum cell manipulation, under *in vivo* condition, and with minimum influence of any external force, torque and pressure. Finally, we have also elaborated on the possible scenario to explain how naturally deformed bacteria are formed from initial to final-stage.

Keywords bacteria · *Escherichia coli* (*E. coli*) · membrane biophysics · microscopic imaging · *in vivo* imaging

1 Introduction

The behavior and survival of bacteria as ancient living organisms in our planet have been interesting subjects for researchers. In view of the fact that the shape of bacteria can be assumed to play an important role in their behavior and survival, scientists have been fascinated by the large variety of cell shapes between different species (Harold 1990; Cooper and Denny 1997; Young 2006, 2007; Dusenbery 2009; Ursell et al 2014). Cell shape is the result of a complicated process and interest in understanding this process has increased by both biological and biophysical approaches (Bendezu et al 2009; Shiomi et al 2008; Margolin 2009; Cabeen and Jacobs-Wagner 2007; Cabeen et al 2009; Sliusarenko et al 2010; Sun and Jiang 2011; Jiang et al 2011;

Department of Nanobiotechnology, Faculty of Biological Sciences, Tarbiat Modares University, Tehran, Iran.
Tel.: +98-21-8288-4410; Fax: +123-45-678910
E-mail: naderman@modares.ac.ir

Huang and Ramamurthi 2010; Wang et al 2010; Huang et al 2006; Zimmerberg and Kozlov 2006; Männik et al 2012; Furchtgott et al 2011; Mukhopadhyay and Wingreen 2009; Ploeg et al 2013; Wang and Wingreen 2013; Ursell et al 2014; Amir 2014; Amir and van Teeffelen 2014; Iyer-Biswas et al 2014; Zaritsky 2015; Vischer et al 2015; Gray et al 2015). Despite intensive research in this area, the mechanisms of auto-regulation and maintenance of cell shape has not completely been solved yet (Huang et al 2008; Furchtgott et al 2011; Mukhopadhyay and Wingreen 2009; Osborn and Rothfield 2007; Olrichs et al 2011; Kawai et al 2011; Typas et al 2012; Amir 2014; Ursell et al 2014; Eun et al 2015; Zaritsky 2015; Zaritsky and Woldringh 2015; Vischer et al 2015; Gray et al 2015; Turner et al 2014; Schirner et al 2014; Nguyen et al 2015).

Previous cell shape studies have shown that *Escherichia coli* (*E. coli*) generally looks like a rod with two symmetric hemispherical caps but, the recent study (Itan et al 2008) reported the first *in vivo* observation of spatial heterogeneity over one hundred *E. coli* cells of a specific strain (*in vitro* observation (Vardi and Grover 1992, 1993)).

Based on the existence of the irregular non-rod-shaped cells (spatial heterogeneity in cell shape) both experimentally (Itan et al 2008) and theoretically (Huang et al 2008), we focus on one type of non rod-shape which we name bent-shape. From a physicist point of view, we *assume* that cell shape configurations of *E. coli* represent a two-states system: rod-shape as a native state and bent-shape as a perturbed state. We ask a simple and fundamental question, whether the difference between energies of native (rod-shape) and perturbed (bent-shape) states can be estimated? Answering this question would help researchers to better understand the reason of forming these naturally perturbed cell shapes and may also shed light on the auto-regulation mechanism and intra-cellular regulation of shape in rod-shaped bacteria.

We used a deflagellated non-motile strain of *E. coli* in the steady-state growth condition (Zaritsky et al 2000; Grover and Woldringh 2001), and by applying the digital-camera-microscopy, *E. coli* cells were classified. Then, we calculated the probability of occurrence of various shapes of bacteria in order to verify (our assumption) the two-state system. Our cell growth method was not similar to Ref. (Itan et al 2008), but we obtained similar results, *i.e.* the most probable configuration of *E. coli* cell is the rod-shape. Following that, we developed an energetic approach and, from the geometrical data (image processing) we estimated the payoff energy to deform a rod-shaped *E. coli* cell to a bent-shaped cell with the same radius of end-caps and the same length. Since in general, the deformation could be due to bending, shearing and stretching, we determined the contribution of bending, shearing and stretching, to the energy cost of three layers of the cell's envelope in a bent-shaped bacterium.

To our knowledge, our analysis provides the first estimate of the energy necessary to make a bent-shaped cell. By considering the experimental condition, the estimated energy is at the order of 10^{15} $k_B T$ per bacterium. Finally, based on the observation of bent cells and the calculated energy necessary for bending, we can ask where, when and how the bending occurs? Following that, we studied a mechanism of the bent-shape formation and we think the key to understand what is going on could be found, by studying the subject of "deformation of a new-born rod-shaped cell into a bent-shaped cell" rather than the subject of "deformation of a rod-shaped cell to

a bent-shaped cell". We suggest a probable mechanism of bent-cell formation by considering "the dynamics of synthesizes of the peptidoglycan layer" of a new-born rod shaped cell.

2 Experimental Procedures

We have used the mutated *E. coli* strain HCB137, which was obtained kindly from K. Fahrner, Department of Molecular and Cellular Biology, Harvard University, Cambridge, MA. The strain HCB137 is not motile because it lacks the entire flagella (Δ(*flhC-flhA*)). Stock cells were taken from the refrigerator and after an overnight growth on the agar plate, cells were inoculated in the pre-warm fresh medium of TY medium (10 g tryptone, 5 g yeast extract, and 5 g of NaCl per liter, and *p*H=7). For the first 5 dilutions, the doubling time of the growth at 21 °C in the TY medium ($T_D \simeq 110 \pm 17$ min) was considered as was measured before (Tavaddod et al 2011) and at optical density about 0.4-0.6 (at 455 nm), the bacterial culture was inoculated to a new flask with fresh pre-warmed TY medium. Since starting of the dilution procedure should be done before the beginning of the stationary-phase, we needed to recognize the proper time of dilution at optical density 0.4-0.5. Therefore, in each inoculation, the growth curve was prepared in parallel with each culture flask. This process was followed at least 20 times (generations) to achieve a "homogeneous" bacterial culture. Then, samples for imaging were taken at the optical densities 0.1-0.3.

We pipetted a drop of $3.5 - 4 \pm 0.5$ μl bacterial culture in the desired density onto a clean microscope slide. The cells are immobilized by attachment to the glass surface by a clean coverslip (with 22mm × 22mm surface area) which was gently placed on top of the drop. In fact, in some preparations the cells were not immobilized by attachment and kept moving in TY medium and that in others they would attach, for unknown reasons, to the glass surface. It were the latter preparations that we used for imaging. In order to prevent shrinkage of cells or any additional probable change in the shape of cells due to evaporation of liquid, the chamber was quickly sealed with VALAP (equal weight of Vaseline, Lanolin, and Paraffin). The resulting depth of the chamber is about 6-9 μm. All experiments were performed at room temperature.

For cell observation an inverted phase-contrast microscope (IX81, Olympus) with a 100×, 1.4 NA phase oil objective was used. Images were recorded with a digital-camera (DP72, Olympus).

The images taken in the TIF mode, consist of 1360×1024 pixels. They were taken from different parts of the chamber (See Figs. 1A and 1B) which means one snap shot of the field of view of the digital-camera and far from the edges. It appeared that the lengths of the attached cells were always in the focal plane of observation. In this case, it might be possible to assume the surface area of the confined cells are imaged in snap-shots. Since the chambers are filled with bacterial culture, while doing digital-camera-microscopy, the cells are alive and continue to grow. However, in order to avoid cells going into stationary phase due to lack of oxygen, all images were recorded within 20 min after chamber preparation. All the studied images were belonged to cell culture flasks which were diluted periodically in 1.2 days. Image

processing and analysis has been performed using Matlab (The MathWorks, Natick, MA). Image analysis has been done at sub-pixel resolution similar to the method used in PSICIC of Guberman *et al.* (Guberman et al 2008).

To determine the edge position, at first a binary threshold value has been set. To overcome the roughness problem due to the pixilated border, we used the method of interpolation of contours (Guberman et al 2008). This method is based on choosing the specific threshold and it causes less sensitivity to find the total area of a bacterium. Unlike PSICIC (See Ref. (Guberman et al 2008)), our image processing code has a limitation in finding the contour for more than one cell in an image. To overcome this problem, we have defined a region of interest within the size of a typical bacterium and we discard data from those cells that are too close to each other. The positions of poles, center of mass (CM), area, long and short axes, cell border in internal coordinate system are extracted from the images of bacteria with different lengths (Guberman et al 2008). The final spatial resolution of the digital optical imaging is 34 nm, along each direction. The interpolated contour which was obtained with PSICIC method contains a series of discrete points around the cell with $1-5$ nm spatial resolution both horizontally and vertically.

3 Results

Generally, *E. coli* looks like a capped cylinder and can be approximated by three zones (See Fig. 1D) and two of them correspond to two caps at both ends of a cell. We label the zones as left cap and right cap (right and left as observed by reader) and the area between two caps is the cylindrical-zone. Since *E. coli*'s elongation happens mainly along the side wall (naturally in a homogenous bacterial culture), the length of a cell is in the range of $\langle L_{\text{newborn}} \rangle \leq L \leq \langle 2L_{\text{newborn}} \rangle$, where the $\langle \ \rangle$ indicates the average length. For our analysis, the bacteria have been chosen from those cells whose shapes are in the pre-divisional state of growth $L < \langle 2L_{\text{newborn}} \rangle$, which was judged by eye (not showing signs of cell constriction). This is to circumvent the complicatedness of the effect of cell division on the cell's shape.

Observation of a population suggests that the classification of cells could be done based on the geometrical features of symmetric and asymmetric properties. There are two types of asymmetric properties. The "Left-Right asymmetry" (LR-asymmetry) which characterizes the cell whose left cap differs from the right cap (one is smaller than the other). The "Cylindrical asymmetry" (C-asymmetry) which is the property of the cell whose cylindrical region deviates from a straight cylinder.

In order to evaluate and select the LR-asymmetric cells, the position of starting cap zones relative to the associated poles (See Fig. 1D) are measured (R_L, R_R) and the cells whose $R_L = R_R$, are selected as the cells with LR-symmetric property. A careful analysis shows that LR-asymmetric cells contain the C-asymmetric property. This is reasonable by considering the point that we have defined the LR-asymmetry relative to the poles coordinates (for poles detection see Ref. (Guberman et al 2008)) and our finding is in accordance with the previous report (Itan et al 2008). Hence, we classify the cells into two groups in regard to the LR-asymmetry (See Table. 1).

To classify the cells into two groups, a Matlab code is written to analyze the sub-pixel information of the deflagellated cell which was obtained of image processing (described before). We represent the border of each cell by a sequence of points $p_n = (x_n, y_n)$, where $x_n = x(n)$, $y_n = y(n)$, and n denotes the number of discrete points on the border. To indicate the positions of starting cap-zones, we have used the variation of the local-cell-width (w) along the axial direction of a cell (See Fig. 2A). Knowing the variation of the local-cell-width (w) of each cell, enabled us to define the position of the left R_L and right cap R_R, the points which:

$$R_L = \text{Max}[(w(j+3) - w(j)) > 2\delta_{\text{unc}}], \tag{1}$$

where $j = 1, 2, 3, ..., N$, and

$$R_R = \text{Min}[(w(j+3) - w(j)) < -2\delta_{\text{unc}}]. \tag{2}$$

Here, j, N, w and δ_{unc} denote the number of points on the border, total number of the points on the border, the local-cell-width at point j and uncertainty in finding the cap's position. We fixed the total number of the points on the border to 1200, which makes 600 cross section cuts. Uncertainty in finding the cap's position is obtained from dividing the length of each cell by 600. It is reasonable to consider R_L and R_R as radius of the left and right cap, respectively. Fig. 2A shows the local-cell-width along the side wall of the long axis of a cell.

The described data analysis was applied to 509 (N_{Tot}) single cells that had grown in 1.2-days cell cultures (in the steady-state as described before). The cells were picked up for the data analysis which non of 509 cells showed constriction. Based on our analysis, 85% of the cells ($N_{\text{LR-Sy}} = 431$) have the LR-symmetric property (See Fig. 2B and Table. 1). Next, we classified the cells with LR-symmetric property ($N_{\text{LR-Sy}} = 431$) into two groups based on their C-asymmetric property: I) cells with LR-symmetry and C-symmetry (N_{Rod}), and II) cells with LR-symmetry and C-asymmetry (N_{Bent}). To do this, we defined the quantity $\delta_{\text{C-M}}$ as:

$$\delta_{\text{C-M}} = |\delta_C - \delta_M| \qquad \delta = x, y, \tag{3}$$

where δ_C and δ_M are the coordinates of the center of mass, and mean point in the line that connects two poles, respectively. Deviation of $\delta_{\text{C-M}}$ from a threshold value was the reference to select cells with C-asymmetric property (bent-shaped cells). The value of 3 times of the length of a mapped-pixel ($\xi = 3 \times 34$ nm=102 nm) was set as a threshold value in Eq. (3) and bent-shaped cells were selected when $\delta_{\text{C-M}} > \xi$. To verify the right selection of bent-shaped cells, we also measured the radiuses of curvature ($\Re$) in the cylindrical region of all bent-shaped cells, similar to Ref. (Itan et al 2008). The results of finding the bent-shaped cells from the two methods almost were the same and we could increase the sensitivity of bent-shape-detection into $\delta_{\text{C-M}} > \xi = 2.4 \times 34$ nm$\simeq$80 nm.

The bent-shape detection was applied on only cells with the LR-symmetric property. As it is shown in Fig. 2C, the length of analyzed cells (with LR-symmetric property, $N_{\text{LR-Sy}} = 431$), varies from 1-3.8 μm. But, only cells number in the length ranges of 1.4-1.8 μm, 1.8-2.2 μm, and 2.2-2.6 μm are enough to statistically analyze them. Due to relatively high population ($N_{\text{LR-Sy-SL}} = 211$) of bacteria with almost the

same length ranging from 1.8 μm to 2.2 μm, we performed the rest of analysis on cells number in the mentioned length ranges. Finally, 80% of the LR-symmetric cells "with the same radius of end-caps and the same lengths" showed the rod-shape and 20% of the cells the bent-shape (See Figs. 2B-C and Table 1). Although we used a different method of cell growth as compared to Ref. (Itan et al 2008), we obtained similar results indicating the most probable configuration of *E. coli* cell is the rod-shape. Besides that, the probability of occurrence of bent-shape is not low enough to neglect it. Regarding the geometrical features of cell shape in our experiment, it is possible to suggest a "two-state system for cell-shape"; native state (rod-shape) and perturbed state (bent-shape). The next step is to know the difference between energies of rod-shape and bent-shape.

4 Discussion: Energy to Deform Envelope Layers

In general, the deformation of cells could be due to bending, shearing and stretching. The cell envelope is composed of three different structures: an outer membrane (OM), an inner membrane (IM) and a peptidoglycan (PG) layer (Ruiz et al 2006). The inner membrane (IM) is a symmetric bilayer of phospholipid, while the OM is an asymmetric bilayer of lipopolysaccharides in its outer leaflet (Ruiz et al 2006). The periplasmic space is composed of a gel-like carbohydrate-rich polymer which is more viscous than the cytoplasm (Silhavy et al 2010) and the peptidoglycan layer (PG). Braun's lipoproteins (BLPs) tightly link the OM to the PG layer by covalent bonds. The hydrophobic heads of BLPs are embedded in the OM. This linkage of two layers is done by more than $500,000$ Braun's lipoproteins (Silhavy et al 2010). In the work of Jauffred *et al.*, they suggested that a force is needed to overcome the adhesion of the OM to the PG layer (from the extracted elastic OM tethers by optical tweezers) (Jauffred et al 2007). Hence, it is reasonable to assume that BLPs act as large number of pins which randomly pin the OM to the PG network. With these adhesions of the OM to the PG layer, the deformation of the stiffer layer which is the PG layer, dictates the type and pattern of the deformation to the relatively softer layer (OM). Now, in the following paragraphs we use the raw data of the image analysis and with energetic approach try to estimate (calculate) in three layers of the cell envelope, does the contribution of energy cost to form a rod-shape into bent-shape, belong to the stretching energy or bending energy? In our experiment, it is reasonable to neglect the shearing deformation in the PG layer and in both the IM and OM.

The peptidoglycan mesh is constructed from strands of merely unstretchable glycans which are cross-linked by relatively stretchable polymer peptides (Boulbitch et al 2000). The glycan filaments wrap around the circumference of the cylinder and peptides crosslink between pairs of glycan in longitudinal direction. Due to the high turgor pressure (1 atm (Deng et al 2011)) and the low resistance of the PG bonds, it is reasonable to neglect the bending energy of the PG layer so that the contribution of energy cost to deform the PG layer is only to be ascribed to stretching energy (Lan et al 2007; Sliusarenko et al 2010; Arnoldi et al 2000).

In order to estimate the stretching energy of the PG layer in a deformed bent-shaped bacterium, we estimate the primary mechanical stresses of 1) radial stress,

and 2) axial stress in a deformed cylinder. We neglect the PG contraction in the other directions, if we pull/push the PG layer in one direction (the Poisson effect).

There is an anisotropy in the Young's modules of the PG layer, $Y^{\text{Pep}} = \frac{1}{2}Y^{\text{Gly}}$, where Y^{Pep} and Y^{Gly} are the Young's modules of peptide and glycan filaments, respectively (Yao et al 1999). Hence, it is easy to deform (stretch) a peptidoglycan network along the longitudinal direction in comparison to the circumferential direction.

At the simplest model, we may assume that the PG bonds do not stretch in radial direction and during the formation of the bent-shape, the cells are not subjected to the extensional strain ε_r from the longitude symmetric axis y (See Fig. 3). Therefore, for simplicity in energy calculation/estimation, we may consider the bent-shape as a deformed rod-shape that has not been deformed in the radial direction ($\varepsilon_r = 0$). However, as Fig. 2D shows, comparison of the probability distribution function of the cell width of 211 analyzed cells with the same length shows a significant difference in the "mean" width of the bent-shaped cells in comparison to the "mean" width of the rod-shaped cells which is not consistent with constant bacterial width in the steady-state growth condition. We observed cells (those were with almost the same length ranging from $1.8 - 2.2$ μm) with a large width (0.7-0.8 μm) in particular show more bent-shaped cells. Perhaps this is comparable to the width-increase at the constriction site occurring during nutritional shift-up as described in (Woldringh et al 1980).

Because we compare the energies of a rod-shape and a bent-shape within cells with the same "length", it is reasonable to consider only the contribution of the mechanical axial stress in the PG mesh of a deformed bent-shape cell. From the energetic point of view, we only face with stretching energy along the axial direction. In the microscopic view, we assume bonds between PG mesh structure above the symmetry axis (y) are stretched while those below the symmetry axis are compressed (See Fig. 3). Since the thickness of the PG layer (h^{PG}) and the mean width of an *E. coli* bacterium ($\langle w \rangle$) are about $2 - 4$ nm (Gumbart et al 2014), and 600 nm (based on our measurement), respectively, then:

$$\langle \frac{h^{\text{PG}}}{\langle w \rangle} \rangle \approx 0.006 \ll 0.1. \tag{4}$$

Hence, it is reasonable to assume the PG layer as a "thick-walled" cylinder. Therefore, the axial strain $\varepsilon_L = \varepsilon_y$ which is a measure of the fractional extension is:

$$\Delta\ell = d\ell_2 - d\ell_1 = (\Re + r)\varphi - (\Re - r)\varphi \approx w\varphi, \tag{5}$$

$$\varepsilon_L = \frac{\Delta\ell}{L - (R_R + R_L)} = \frac{w\varphi}{\Re\varphi} = \frac{w}{\Re}, \tag{6}$$

where r ($r = w/2$), L, $L - (R_R + R_L)$, and $\Re$, are the half of the cell-width, the length, the cylindrical part of the cell, and the radius of the curvature in a bent-shaped cell, respectively. Therefore, the axial strain inversely relates to the radius of curvature. Here, $\Delta E_{\text{Str}}^{\text{PG}} = E_{\text{Bent}}^{\text{PG}} - E_{\text{Rod}}^{\text{PG}}$ is the required energy to deform the PG layer of a rod-shaped cell into a bent-shaped cell without changing the length of the cell. Given the

strain within the cylindrical part of the a bent-shaped cell ε_L, and using Hook's law, we estimate the strain energy density $\mathscr{E}^{\mathrm{PG}}$ which is given by:

$$\Delta \mathscr{E}^{\mathrm{PG}} \; = \; \frac{1}{2} Y_L \varepsilon_L^2 \; = \; \frac{2 Y_L r^2}{\mathfrak{R}^2}, \tag{7}$$

where Y_L is the Young's modulus in the axial direction, $Y_{\mathrm{L}} = Y^{\mathrm{Pep}} \sim 30$ MPa (Deng et al 2011; Amir et al 2014). From the experimental data of 42 bent-shaped cells, the axial stretching strain in axial direction of the PG layer is estimated as $\langle \varepsilon_L \rangle = \frac{\langle w \rangle}{\mathfrak{R}} \approx 0.14$. Then, the mean energy density for stretching the PG layer is $\Delta \mathscr{E}^{\mathrm{PG}} \approx 0.3$ MPa, which is given $\Delta E_{\mathrm{Str}}^{\mathrm{PG}} = 7 \times 10^7 \; k_B T$ required to stretch a 1 nm^2 of the PG layer, where k_B is the Boltzmann constant and T is the temperature. In a larger volume of the deviated part of the bent-shape, given the length of the cylinder $\ell_{\mathrm{Bent}} = L - R_R - R_L \approx \langle L \rangle - \langle w \rangle = 2 - 0.6 = 1.4 \; \mu$m, the typical deformed PG area is about $S^{\mathrm{PG}} = 2\pi \langle r \rangle \ell_{\mathrm{Bent}} \sim 2.6 \times 10^6$ nm^2. It leads to $\Delta E_{\mathrm{Str}}^{\mathrm{PG}} \sim 10^{15} \; k_B T$ to stretch the cylindrical part of a rod-shaped bacterium to a bent-shape and is a huge high cost of energy per bacterium. To give a feeling for this amount, bending a 1 μmm elastic rod with an aspect ratio of 20:1 into a semicircular arc costs about $10^{12} \; k_B T$ (Phillips and Quake 2006).

Indeed, we supposed the axial strain in the PG layer is a constant value in the whole deviated part of the bent-shape while near mid-cell, the PG layer is under highest stress. Therefore, this is not a complete assumption and the real value of the energy cost to stretch the PG layer should be smaller than what we estimated here.

Besides that, a very interesting study has revealed that the PG layer is a porous network with a pore-size distribution varying from 4-16 nm (Turner et al 2013) which could largely decreases the required energy.

Next point that should be noted is, we used the Hook's law while previous interesting experimental and theoretical studies (Deng et al 2011) have shown that the PG layer is a stress-stiff polymer network and the stiffness of the PG layer depends on the applied stress. In the bent-shaped cell, the axial strain ε_L, is due to an applied stress, and the mentioned stress changes the global elasticity of the PG layer (Deng et al 2011), and it should be considered in the further study.

Pinning OM onto PG layer with more than $500,000$ Braun's lipoproteins gives an estimation of presence of more than $350,000$ BLPs in the cylindrical part ($\ell_{\mathrm{Bent}} = L - R_R - R_L \approx \langle L \rangle - \langle w \rangle = 2 - 0.6 = 1.4 \; \mu$m) of a bent-shaped cell. If we assume (Zaritsky et al 1979) the surface density of BLPs is nearly constant on the surface area of a typical bacterium with the length of $\langle L \rangle = 2 \; \mu$m, then in average, the area of four neighbors BLPs is about 2.7×2.7 nm^2. Hence, it seems, due to the presence and pinning OM into PG layer, the stretched PG layer dictates a deviation on the OM-bilayer which is not a single arc. Probably, there are on average nearly $300,000$ localized mini-arcs as a substructure with an average area of 2.7×2.7 nm^2 for each localized mini-arc. We start to estimate what is the payoff energy to create each mini-arc. From the energetic point of view, since the end of BLPs covalently binds into the PG layer, a stretch in the PG layer forces each mini-OM-bilayer (which is in cages of four neighbors BLP) to stretch itself. From the experimental data of 42 bent-shaped

cells, the axial stretching strain in axial direction of the PG layer is estimated as $\langle \varepsilon_L \rangle = \frac{\langle w \rangle}{\langle \Re \rangle} \approx 0.14$. We supposed that the axial strain in the PG layer is a constant value in whole of the deviated part of the bent-shaped cell which is reasonable for a first estimation. Then, we may assume each mini-OM-bilayer is subjected to roughly the same axial strain of the PG layer. Using the bending modulus of $\kappa_b \sim 20\ k_B T$ for a typical bilayer, gives an estimation of $Y_{\text{Str}} \sim 60\ k_B T/\text{nm}^2$ for Young's (stretching) modulus of the OM-bilayer in the axial direction through the equation:

$$\kappa_b = \frac{1}{48} Y_{\text{Str}} (h^{\text{OM}})^2, \qquad (8)$$

where $\langle h^{\text{OM}} \rangle \approx 4$ nm (Beeby et al 2013), is the thickness of the OM-bilayer. Then, using $\Delta \mathscr{E}^{\text{OM}} = \frac{1}{2} Y_L \varepsilon_L^2$ results in the mean payoff energy density $\Delta \mathscr{E}^{\text{OM}} \sim 0.6\ k_B T/\text{nm}^2$. Hence, for a typical mini-OM-bilayer, the mean payoff energy $\Delta E^{\text{OM}}_{\text{Str}} \sim 4.5\ k_B T$ is estimated which is not a high cost of energy and attainable easily through the thermal energy. Considering the asymmetry in composition of the OM-bilayer and population of other proteins in the OM-bilayer, can decrease the bending modulus of κ_b to an effective value smaller than what we used here. Following that, the required energy to deform each mini-OM-bilayer decreases to a few $k_B T$ which is at the order that easily through the thermal energy is attainable. Hence, shape fluctuations in the OM at a mini-OM-bilayer scale could occur as a result of the fluctuation in thermal energy. The existences and fluctuation in shape of the mini-OM-bilayer could be investigated in future studies.

There is no evidence about a physical attachment or any other specific strong interaction between the PG layer and IM. The surface area of the IM can not be larger than the surface area of the PG layer. It is not clear yet, but probably the IM in a bent-shaped cell has a similar shape to the envelope of the bent-shaped cell and we estimate what the payoff energy is to break the C-symmetric in the IM of a bent-shaped cell whose cylindrical part deviates $\xi = 2.4 \times 34 \simeq 80$ nm. Using bending modulus of $\kappa_b \sim 20\ k_B T$ for the IM, the mean payoff energy of deviating the cylindrical part of a bent-shaped cell when $\Re \sim 10\ \mu$m, is estimated $\Delta E^{\text{IM}}_{\text{Bent}} = 6\pi \kappa_b \frac{\xi}{\Re} \sim 8\ k_B T$, which is not a high cost of energy and attainable easily through the thermal energy. In a similar manner to the OM, considering the population of other proteins in the IM, can decreases the bending modulus of κ_b to an effective value smaller than what we used here. Therefore, the required energy to deform the IM decreases to a smaller value that we estimated here.

Finally, in order to form a rod-shaped bacterium into a bent-shaped cell whose cylindrical part deviates $\xi = 2.4 \times 34 \simeq 80$ nm, one has to payoff $\Delta E_{\text{Tot}} = E_{\text{Bent}} - E_{\text{Rod}} \sim 10^{15}\ k_B T$, to stretch the PG and OM, and bend the IM. By considering the experimental condition, it is clear that there is not an external source of energy at the order of $\Delta E_{\text{Tot}} \sim 10^{15}\ k_B T$ per bacterium. Now, the question which comes is, with such a huge amount of energy cost in forming a rod-shaped cell into bent-shaped cell, why are approximately 20% of the cell population still has bent-shape?

We believe that the key to understand the process is to consider "the dynamics of PG layer" during growth of a single bacterium.

Huang *et al.* discussed the existence of the other possible shapes (i.e. cracked cell with a bulge or helical cell shape) of a rod-shaped bacterium by modeling the peptidoglycan cell-wall as a 2D spring network. They showed that the shape we have named bent in our study, is the results of removing a single peptide of the PG layer "at the mid-cell" of a rod-shaped cell (Huang et al 2008). They could successfully predict the "existence" of the bent-shape, but they did not consider the growth and synthesis of the PG layer in their model.

We start by estimating whether the probability of occurrence of a defect in the PG layer "near the mid-cell" is increased or not (during the growth and synthesis of PG layer)? The average cost of energy to break a peptide is estimated about $3-5\ k_B T$ (a covalent bond) which could be easily obtained through the thermal energy. Hence, globally, shape fluctuations in the PG layer at the order of a single peptide length could easily occur. Moreover, during cell growth, the synthesis of the PG layer is done by elongation when the penicillin binding proteins (PBP) break and link new strands into the PG layer "near the mid-cell" (Lan et al 2007; Laloux and Jacobs-Wagner 2014). Thus, the process of the synthesis of the PG layer (besides the thermal energy) also might cause a defect in the PG layer "near the mid-cell". Besides that, it might be possible that during the cell-wall synthesis, an extra internal stress component–even in a short time interval–affects the PG layer and also makes defects in the PG layer. For example, FtsZ-ring as a force generator (Wang and Wingreen 2013) would be a proper candidate or indirect interaction of nucleoid via polyribosomes (Woldringh (2002); Rabinovitch et al (2003)). Therefore, the thermal energy together with the synthesis of the PG layer (during cell growth) mainly increase the probability of occurrence of a defect "near the mid-cell" in comparison to the other part of a cell. Regardless of the reason(s) of the defect-creation, a recent report has revealed that in the Gram-negative bacteria, the PG layer is more disordered than previously thought and that the pore-size distribution varies from 4-16 nm (Turner et al 2013). From the other side, according to the recent studies (Nelson 2012; Amir and Nelson 2012; Amir et al 2014), a Peach-Koehler force acts between a couple of defects and dislocations (long-range elastic interactions between dislocations) in the PG layer and causing a mechanical stress. Since chemical reaction rates are typically sensitive to force (stress), there will be a coupling between the mechanical stress and the PG layer synthesize (chemical reaction). The mechanical stress due to the Peach-Koehler force increases the speed of processive motion of the strand elongation machinery (Nelson 2012; Amir and Nelson 2012). Also, local elastic stress increases the activation energy of insertion of new glycan strands (nucleation) (Lan et al 2007; Nelson 2012; Amir and Nelson 2012; Amir et al 2014). Hence, all together, we think, the defects in the PG layer of a new born rod-shaped cell that we named initial-stage, forces the PG layer to synthesis in a wrong and deviating direction.

From a macroscopic point of view, considering the results of the recent experiment on the plastically deformed bacteria (Amir et al 2014), together with the C-asymmetry in our selected bent-shaped bacteria, have brought us to the point that probably in the new born rod-shaped cell, the Peach-Koehler forces affect the PG layer synthesizes as a localized effective force **F** during the cell growth. Then, it (**F**) forces the PG layer to synthesize in a wrong direction and causes a cell shape with the C-asymmetry property. We think, the effective force (**F**) probably affects in a

short time interval $0 < t \ll t_d$, which is much lower than the doubling time t_d of the bacterium as:

$$F(t) = \begin{cases} F & \text{if } 0 < t \ll t_d \\ 0 & \text{otherwise.} \end{cases}$$

From the geometry of the bent-shaped cell (See Fig. 3), in the simplest model, the deformation could be due to a radially inward force $\mathbf{F} = F(-\hat{r})$ which should be perpendicular to the bacterial axis of symmetry (y direction in Fig. 3).

One could consider the kinetics of the PG layer synthesis similar to the approach in Ref. (Lan et al 2007) in a new born rod-shaped cell and in the presence of a force in a short time, and gives a mechanism and quantitative description of the PG growth and formation of a bent-shaped cell.

The final point that we would like to discuss about it in the bent-shaped cell is, if the Peach-Koehler forces due to the defects in the cell wall are responsible for the wrong direction of the PG layer-synthesizes, why do not the cytoskeleton MreB filaments as a local sensor of the curvature in *E. coli*'s envelope (Ursell et al 2014; Schirner et al 2014), regulate the cell shape into rod? We think, probably, the number and size of the defects could be critical in the formation of the bent-shaped cell. These factors could play main roles to answer why approximately 20% of the bacteria that grow in the similar condition with the other rod-shaped cells, are deformed to bent-shape, and approximately 80% of cells could escape of this deformability.

Apart from the candidate mechanism of bent-cell formation, in order to know experimentally the physical nature of this deformability in the cylindrical part of the cell, we recorded a series of time-lapse snap-shots within 5 min. The deformation in our experiment does not reverse due to the fluctuation in the thermal energy. We did not observe any transition between these two states of rod-shape and bent-shape within a single cell and changes in shape from the rod to the bent-shape are not due to thermal fluctuations. Since the PG layer as a major structure of the cell shape relatively has an elastic mechanical structure (Lan et al 2007), we think that probably at a very short time scale, the mechanical features of bacterial cell shape (cell envelope) is more elastic while at a longer time scale comparable with its doubling time, more plastic property will dominate. Probably after small amount of the deformation with elastic property, some cardiolipin lipids (Sliusarenko et al 2010; Mukhopadhyay et al 2008; Renner and Weibel 2011), proteins which are sensitive to the curvature (Laloux and Jacobs-Wagner 2014) and MreB as a local sensor of the curvature (Ursell et al 2014; Schirner et al 2014) bind and localize to the deformed part and consequently, will cause the plasticity nature of the deformation.

5 Conclusion

The present study describes a physical approach to the probable reasons of forming naturally perturbed cell shapes and may shed light on the auto-regulation mechanism and intra-cellular regulation of shape in the rod-shaped bacteria.

Obtaining the conformation-space of the number of *E. coli* cells (in the steady-state growth condition) gives a better idea of what the most probable shape-state of a strain of *E. coli* as a model organism in the rod-shaped bacteria is. From the

probability of occurrence of each shape-state, we suggested a two state system. Rod-shape which is the most probable state as a native state and bent-shape as a perturbed state.

In order to estimate what the difference between two state systems of *E. coli*'s shape is, we have applied an energetic approach in cell shape study. Extracting geometrical data by image processing has helped us to elaborate on the shapes from the energetic point of view. The estimated energy is much higher than it could be easily attainable (10^{15} $k_B T$ per bacterium). We think the key to understand what is going on is, considering a new born rod-shaped bacterium is deformed to a bent-shape rather than deformation of a rod-shape to a bent-shape. We offer a possible scenario for "initial-stage" of bent-shape formation of a new born rod-shaped cell. Due to 1) the low cost of energy ($3 - 5$ $k_B T$) to break a peptide which could be easily obtained through the thermal energy, and 2) the mechanism of the break peptide near the mid-cell by penicillin binding proteins, the probability of occurrence of a defect near the mid-cell in comparison to the other part of a cell is increased. Then, Peach-Koehler forces act between defects and result in mechanical stress in the PG layer and the speed of processive motion of the strand elongation machinery increases (Nelson 2012; Amir and Nelson 2012; Amir et al 2014). Hence, we think, the defect formation in the PG layer of a new born rod-shaped cell forces the PG layer to synthesize in a deviated direction. Probably, the number and size of the defects could be critical in the formation of bent-shaped cells and play a main role to why approximately 20% of the bacteria in the same length range who are grown in the similar condition with the other rod-shaped cells are deformed to bent-shape and 80% (under resolution of our experiment) could escape of this deformability. Indeed, in finding the type of deformation in each layer of the cell envelope, we *assumed* the cell envelope consists of the similar building blocks everywhere around the cell even in caps. Besides that, we have supposed that it is possible to neglect of shearing and isotropic compression in the envelope of *E. coli* during our experiment. We assumed all the cells experience the same external osmotic pressure and thus change in shape is not due to an osmotic change. In reality, these are not perfect assumptions (Mukhopadhyay et al 2008; Huang and Ramamurthi 2010; Renner and Weibel 2011) but, in light of accuracy in our experiment these are reasonable assumptions.

Considering the advantages of our experiment which are 1) under *in vivo* condition and 2) it is without any external manipulation, overcomes the lacks which are mainly results of the sub-pixel nanometer analysis in geometrical features of cells. Indeed, more work is needed to fully understand the fascinating problem of naturally plastic deformed bent-shaped cell.

Furthermore, we think the possible scenario for the "stability" of the bent-shaped cell, could be due to the binding of MreB filament, or cardiolipin lipids in negative curvature part of the deformed cell envelope, lead to form a stable bent-shape (plastic deformation). It will be interesting to investigate after forming a cell to bent-shape, whether the outward central curvature in the cylindrical region of non-dividing *E. coli* is a domain which especial proteins (Laloux and Jacobs-Wagner 2014) or cardiolipin lipids are localized (Sliusarenko et al 2010; Mukhopadhyay et al 2008; Renner and Weibel 2011; Laloux and Jacobs-Wagner 2014), or it is a part of MreB (Ursell et al 2014; Schirner et al 2014) or FtsZ (Wang and Wingreen 2013) filaments which are
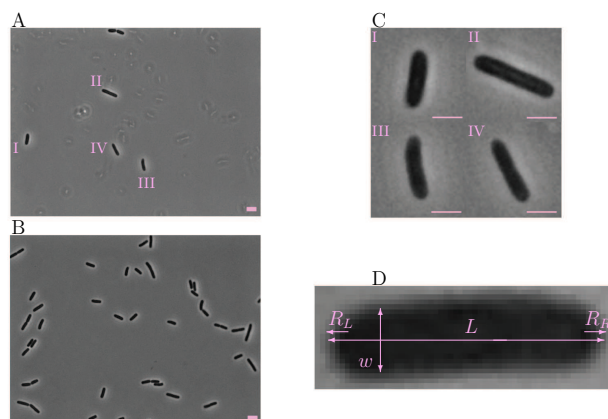
Fig. 1 A typical phase-contrast image of HCB137 *E. coli* cells contains A) a few cells, and B) a large cell number (per the same area and from the same culture flask but from different places of a chamber). C) A larger view of Fig. 1A indicates cells with different morphology. D) L, w, R_L and R_R indicate the length, width, radiuses of left and right caps of the cell. The horizontal scale bars represent 1 μm in A-C images.

Table 1 The results from the geometrical analysis of the *E. coli* images. The range of length in the category of cells with "the same length range" is 1.8-2.2 μm. The length is defined as the length of a cell with the caps (see Fig. 1D).

Cell Shape Property	Number of Cells
Total cells	509 (N_{Tot})
Cells with LR-symmetry	431 ($N_{\text{LR-Sy}} \sim 85\% N_{\text{Tot}}$)
Cells with LR-symmetry (same length range)	211 ($N_{\text{LR-Sy-SL}} \sim 41\% N_{\text{Tot}}$)
Cells with LR and C-symmetry (same length range)	169 ($N_{\text{Rod}} \sim 80\% N_{\text{LR-Sy-SL}}$)
Cells with LR and C-asymmetry (same length range)	42 ($N_{\text{Bent}} \sim 20\% N_{\text{LR-Sy-SL}}$)

in contact with cytoplasmic side of the membrane. We suggest testing this scenario via *in vivo* imaging of cardiolipin lipids-labeled and other possible proteins in the bent-shaped cell for evidence of the interaction protein-lipid. Also, it would be interesting to elaborate on the fine structure of the PG layer in the bent-shaped cell. However, some other could continue the work to study the effect of the cell length on the bent-shape formation. Finally, the spatial distribution of BLPs in our model is quite simple. It would be interesting to study the pinning of OM to the stretched PG layer with BLPs and probable evidence of the mini-OM-bilayer which is a substructure of localized mini-arc.
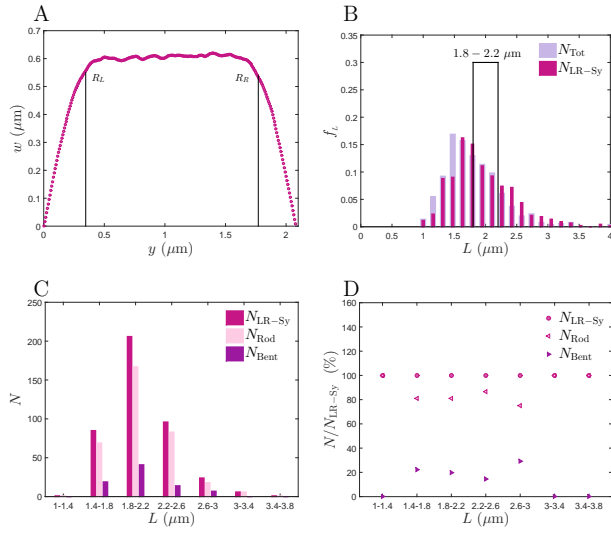
Fig. 2 A) Variation of the local-cell-thickness (w, see Fig. 1D) along the axial direction (y) of a rod-shaped cell. B) The probability distribution function (f_L) of length (L) of total cells (N_{Tot}=509) and cells with LR-symmetry (N_{LR-Sy}=431). The length is defined as the length of a cell with the caps (see Fig. 1D). From the 431 cells with LR-symmetry, 211 cells were in the length range of $1.8 - 2.2$ μm. C) Variation of number of LR-symmetric cells (N_{LR-Sy}), rod-shaped cells (N_{Rod}), and bent-shaped cells (N_{Bent}) based on the length. D) The probability distribution function (f_w) of cell-width (w) of LR-symmetric cells ($N_{LR-Sy} = 211$) were in the length range of $1.8 - 2.2$ μm, rod-shaped cells (N_{Rod}), and bent-shaped cells (N_{Bent}) based on the cell-width.

References

Amir A (2014) Cell size regulation in bacteria. Physical Review Letters 112(20):208,102

Amir A, Nelson DR (2012) Dislocation-mediated growth of bacterial cell walls. Proceedings of the National Academy of Sciences 109(25):9833–9838

Amir A, van Teeffelen S (2014) Getting into shape: how do rod-like bacteria control their geometry? Systems and synthetic biology 8(3):227–235

Amir A, Babaeipour F, McIntosh DB, Nelson DR, Jun S (2014) Bending forces plastically deform growing bacterial cell walls. Proceedings of the National Academy of Sciences 111(16):5778–5783

Arnoldi M, Fritz M, Bäuerlein E, Radmacher M, Sackmann E, Boulbitch A (2000) Bacterial turgor pressure can be measured by atomic force microscopy. Physical Review E 62(1):1034

Beeby M, Gumbart JC, Roux B, Jensen GJ (2013) Architecture and assembly of the gram-positive cell wall. Molecular microbiology 88(4):664–672

Bendezu FO, Hale CA, Bernhardt TG, de Boer PA (2009) Rodz (yfga) is required for proper assembly of the mreb actin cytoskeleton and cell shape in e. coli. The EMBO journal 28(3):193–204
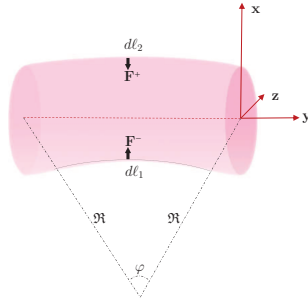
Fig. 3 A cylindrical coordinate system where $\Re$ is the radius of the curvature in the bent-shape.

Boulbitch A, Quinn B, Pink D (2000) Elasticity of the rod-shaped gram-negative eubacteria. Physical review letters 85(24):5246

Cabeen MT, Jacobs-Wagner C (2007) Skin and bones: the bacterial cytoskeleton, cell wall, and cell morphogenesis. The Journal of cell biology 179(3):381–387

Cabeen MT, Charbon G, Vollmer W, Born P, Ausmees N, Weibel DB, Jacobs-Wagner C (2009) Bacterial cell curvature through mechanical control of cell growth. The EMBO journal 28(9):1208–1219

Cooper S, Denny MW (1997) A conjecture on the relationship of bacterial shape to motility in rod-shaped bacteria. FEMS microbiology letters 148(2):227–231

Deng Y, Sun M, Shaevitz JW (2011) Direct measurement of cell wall stress stiffening and turgor pressure in live bacterial cells. Physical Review Letters 107(15):158,101

Dusenbery DB (2009) Living at micro scale: the unexpected physics of being small. Harvard University Press

Eun YJ, Kapoor M, Hussain S, Garner EC (2015) Bacterial filament systems: towards understanding their emergent behavior and cellular functions. Journal of Biological

Chemistry pp jbc–R115

Furchtgott L, Wingreen NS, Huang KC (2011) Mechanisms for maintaining cell shape in rod-shaped gram-negative bacteria. Molecular microbiology 81(2):340–353

Gray AN, Egan AJ, van't Veer IL, Verheul J, Colavin A, Koumoutsi A, Biboy J, Altelaar MA, Damen MJ, Huang KC, et al (2015) Coordination of peptidoglycan synthesis and outer membrane constriction during escherichia coli cell division. eLife p e07118

Grover N, Woldringh C (2001) Dimensional regulation of cell-cycle events in escherichia coli during steady-state growth. Microbiology 147(1):171–181

Guberman JM, Fay A, Dworkin J, Wingreen NS, Gitai Z (2008) Psicic: noise and asymmetry in bacterial division revealed by computational image analysis at sub-pixel resolution. PLoS computational biology 4(11):e1000,233

Gumbart JC, Beeby M, Jensen GJ, Roux B (2014) Escherichia coli peptidoglycan structure and mechanics as predicted by atomic-scale simulations. Plos Comput Biol 10:1003,475

Harold FM (1990) To shape a cell: an inquiry into the causes of morphogenesis of microorganisms. Microbiological reviews 54(4):381

Huang KC, Ramamurthi KS (2010) Macromolecules that prefer their membranes curvy. Molecular microbiology 76(4):822–832

Huang KC, Mukhopadhyay R, Wingreen NS (2006) A curvature-mediated mechanism for localization of lipids to bacterial poles. PLoS computational biology 2(11):e151

Huang KC, Mukhopadhyay R, Wen B, Gitai Z, Wingreen NS (2008) Cell shape and cell-wall organization in gram-negative bacteria. Proceedings of the National Academy of Sciences 105(49):19,282–19,287

Itan E, Carmon G, Rabinovitch A, Fishov I, Feingold M (2008) Shape of nonsepted escherichia coli is asymmetric. Physical Review E 77(6):061,902

Iyer-Biswas S, Wright CS, Henry JT, Lo K, Burov S, Lin Y, Crooks GE, Crosson S, Dinner AR, Scherer NF (2014) Scaling laws governing stochastic growth and division of single bacterial cells. Proceedings of the National Academy of Sciences 111(45):15,912–15,917

Jauffred L, Callisen TH, Oddershede LB (2007) Visco-elastic membrane tethers extracted from escherichia coli by optical tweezers. Biophysical journal 93(11):4068–4075

Jiang H, Si F, Margolin W, Sun SX (2011) Mechanical control of bacterial cell shape. Biophysical journal 101(2):327–335

Kawai Y, Marles-Wright J, Cleverley RM, Emmins R, Ishikawa S, Kuwano M, Heinz N, Bui NK, Hoyland CN, Ogasawara N, et al (2011) A widespread family of bacterial cell wall assembly proteins. The EMBO journal 30(24):4931–4941

Laloux G, Jacobs-Wagner C (2014) How do bacteria localize proteins to the cell pole? Journal of cell science 127(1):11–19

Lan G, Wolgemuth CW, Sun SX (2007) Z-ring force and cell shape during division in rod-like bacteria. Proceedings of the National Academy of Sciences 104(41):16,110–16,115

Männik J, Wu F, Hol FJ, Bisicchia P, Sherratt DJ, Keymer JE, Dekker C (2012) Robustness and accuracy of cell division in escherichia coli in diverse cell shapes. Proceedings of the National Academy of Sciences 109(18):6957–6962

Margolin W (2009) Sculpting the bacterial cell. Current Biology 19(17):R812–R822

Mukhopadhyay R, Wingreen NS (2009) Curvature and shape determination of growing bacteria. Physical Review E 80(6):062,901

Mukhopadhyay R, Huang KC, Wingreen NS (2008) Lipid localization in bacterial cells through curvature-mediated microphase separation. Biophysical journal 95(3):1034–1049

Nelson DR (2012) Biophysical dynamics in disorderly environments. Annual review of biophysics 41:371–402

Nguyen LT, Gumbart JC, Beeby M, Jensen GJ (2015) Coarse-grained simulations of bacterial cell wall growth reveal that local coordination alone can be sufficient to maintain rod shape. Proceedings of the National Academy of Sciences 112(28):E3689–E3698

Olrichs NK, Aarsman ME, Verheul J, Arnusch CJ, Martin NI, Hervé M, Vollmer W, de Kruijff B, Breukink E, den Blaauwen T (2011) A novel in vivo cell-wall labeling approach sheds new light on peptidoglycan synthesis in escherichia coli. ChemBioChem 12(7):1124–1133

Osborn MJ, Rothfield L (2007) Cell shape determination in escherichia coli. Current opinion in microbiology 10(6):606–610

Phillips R, Quake S (2006) The biological frontier of physics. Physics Today 59(5):38–43

Ploeg R, Verheul J, Vischer NO, Alexeeva S, Hoogendoorn E, Postma M, Banzhaf M, Vollmer W, Blaauwen T (2013) Colocalization and interaction between elongasome and divisome during a preparative cell division phase in escherichia coli. Molecular microbiology 87(5):1074–1087

Rabinovitch A, Zaritsky A, Feingold M (2003) Dna–membrane interactions can localize bacterial cell center. Journal of theoretical biology 225(4):493–496

Renner LD, Weibel DB (2011) Cardiolipin microdomains localize to negatively curved regions of escherichia coli membranes. Proceedings of the National Academy of Sciences 108(15):6264–6269

Ruiz N, Kahne D, Silhavy TJ (2006) Advances in understanding bacterial outer-membrane biogenesis. Nature Reviews Microbiology 4(1):57–66

Schirner K, Eun YJ, Dion M, Luo Y, Helmann JD, Garner EC, Walker S (2014) Lipid-linked cell wall precursors regulate membrane association of bacterial actin mreb. Nature chemical biology

Shiomi D, Sakai M, Niki H (2008) Determination of bacterial rod shape by a novel cytoskeletal membrane protein. The EMBO journal 27(23):3081–3091

Silhavy TJ, Kahne D, Walker S (2010) The bacterial cell envelope. Cold Spring Harbor perspectives in biology 2(5):a000,414

Sliusarenko O, Cabeen MT, Wolgemuth CW, Jacobs-Wagner C, Emonet T (2010) Processivity of peptidoglycan synthesis provides a built-in mechanism for the robustness of straight-rod cell morphology. Proceedings of the National Academy of Sciences 107(22):10,086–10,091

Sun SX, Jiang H (2011) Physics of bacterial morphogenesis. Microbiology and Molecular Biology Reviews 75(4):543–565

Tavaddod S, Charsooghi M, Abdi F, Khalesifard H, Golestanian R (2011) Probing passive diffusion of flagellated and deflagellated escherichia coli. The European Physical Journal E 34(2):1–7

Turner RD, Hurd AF, Cadby A, Hobbs JK, Foster SJ (2013) Cell wall elongation mode in gram-negative bacteria is determined by peptidoglycan architecture. Nature communications 4:1496

Turner RD, Vollmer W, Foster SJ (2014) Different walls for rods and balls: the diversity of peptidoglycan. Molecular microbiology 91(5):862–874

Typas A, Banzhaf M, Gross CA, Vollmer W (2012) From the regulation of peptidoglycan synthesis to bacterial growth and morphology. Nature Reviews Microbiology 10(2):123–136

Ursell TS, Nguyen J, Monds RD, Colavin A, Billings G, Ouzounov N, Gitai Z, Shaevitz JW, Huang KC (2014) Rod-like bacterial shape is maintained by feedback between cell curvature and cytoskeletal localization. Proceedings of the National Academy of Sciences 111(11):E1025–E1034

Vardi E, Grover N (1992) Aggregation of escherichia coli b/r a during agar filtration: Effect on morphometric measurements. Cytometry 13(5):540–544

Vardi E, Grover N (1993) Shape changes in escherichia coli b/r a during agar filtration. Cytometry 14(2):173–178

Vischer N, Verheul J, Postma M, Van_den_berg_van_saparoea B, Galli E, Natale P, Gerdes K, Luirink J, Vollmer W, Vicente M, et al (2015) Cell age dependent concentration of escherichia coli divisome proteins analyzed with imagej and objectj. Name: Frontiers in Microbiology 6:586

Wang S, Wingreen NS (2013) Cell shape can mediate the spatial organization of the bacterial cytoskeleton. Biophysical journal 104(3):541–552

Wang S, Arellano-Santoyo H, Combs PA, Shaevitz JW (2010) Actin-like cytoskeleton filaments contribute to cell mechanics in bacteria. Proceedings of the National Academy of Sciences 107(20):9182–9185

Woldringh C, Grover N, Rosenberger R, Zaritsky A (1980) Dimensional rearrangement of rod-shaped bacteria following nutritional shift-up. ii. experiments with escherichia colibr. Journal of theoretical biology 86(3):441–454

Woldringh CL (2002) The role of co-transcriptional translation and protein translocation (transertion) in bacterial chromosome segregation. Molecular microbiology 45(1):17–29

Yao X, Jericho M, Pink D, Beveridge T (1999) Thickness and elasticity of gram-negative murein sacculi measured by atomic force microscopy. Journal of bacteriology 181(22):6865–6875

Young KD (2006) The selective value of bacterial shape. Microbiology and molecular biology reviews 70(3):660–703

Young KD (2007) Bacterial morphology: why have different shapes? Current opinion in microbiology 10(6):596–600

Zaritsky A (2015) Cell-shape homeostasis in escherichia coli is driven by growth, division, and nucleoid complexity. Biophysical journal 109(2):178–181

Zaritsky A, Woldringh CL (2015) Chromosome replication, cell growth, division and shape: a personal perspective. Frontiers in microbiology 6

Zaritsky A, Woldringh CL, Mirelman D (1979) Constant peptidoglycan density in the sacculus of escherichia coli b/r growing at different rates. FEBS letters 98(1):29–32

Zaritsky A, Woldringh CL, Pritchard R, Fishov I (2000) Surviving escherichia coli in good shape: The many faces of bacillary bacteria in cellular origin and life in extreme habitats. Springer Science & Business Media

Zimmerberg J, Kozlov MM (2006) How proteins produce cellular membrane curvature. Nature Reviews Molecular Cell Biology 7(1):9–19